1 Tripartite Synapses

The concept of tripartite synapses is used to describe the close structural and functional association between astrocytes and synaptic partners. Therefore, a tripartite synapses encompasses the impact of astrocytes on the extracellular space surrounding synapses, modulating synapses formation as well as synaptic function via uptake of neurotrasmitters and delivery of acting signaling molecules.
Indeed, intracellular Ca^{2+} elevations, either induced by spontaneous astrocytic activity or evoked by neuronal firing, can trigger the release of different active substances from astrocytes, the so-called gliotransmitters. These gliotransmitters, include glutamate, can modulate and control neuronal activity in a huge different way, both through activation of pre- and postsynaptic receptors.
Here the focus is the description of presynaptic pathway regulation of glutamate released from astrocyte, described by the following approach: (i) synaptic release model and related neurotrasmittertime course in the extracellular space (ECS), (ii) astrocitytic Ca^{2+}-dependent gliotrasmitter model and gliotrasmitter dynamics in ECS and (iii) the modulation of synaptic release by the presence of astrocytic exocytosis.

Synaptic Model

The TM model describes synaptic release (r_S) by the product of two factors: (i) the probability of neurotransmitter-containing vesicles to be available for release (x_S), and (ii) the probability of such vesicles to be effectively released by an AP (u_S), which correlates with intrasynaptic Ca^{2+} levels and the ensuing state of occupancy (activation) of the Ca^{2+} sensory of synaptic neurotransmitter exocytosis. The time evolution equations for $u_S(t)$ and $x_S(t)$ reads

$$\begin{aligned} \frac{du_S}{dt} &= -\Omega_f u_S + u_0 \sum_k (1 - u_S^-)\delta(t - t_k) \\ \frac{dx_S}{dt} &= \Omega_d(1 - x_S) - \sum_k u_S^+ x_S^- \delta(t - t_k) \\ r_S(t_k) &= u_S^+ \, x_S^- = u_S(t_k^+) \, x_S(t_k^-) \end{aligned} \tag{1}$$

where the delta function denotes an action potential arriving at time t_k, u_S^+ and x_S^- are respectively the value of u_S immediately after a generic spikes and the value of x_S immediately before a generic spikes. Assuming a total vesicular glutamate concentration of Y_T, the released glutamate, expressed as concentration in the synaptic cleft, is then equal to $Y_{rel}(t_k) = \rho_c Y_T r_S(t_k)$, where ρ_c represents the ratio between vesicular and synaptic cleft volumes. The time course of synaptically released glutamate in the cleft (Y_S) depends on several mechanisms, including clearance by diffusion, uptake, and/or degradation. In the simplest approximation, the contribution of these mechanisms to glutamate time course in the cleft may be modeled by a first-order degradation reaction of characteristic time so that:

$$\frac{dY_S}{dt} = -\Omega_c Y_S + \sum_k Y_{rel}\delta(t - t_k) \tag{2}$$

To complete this description the dynamics of presynaptic receptors must be taken into account. The pool of presynaptic receptors target by gliotrasmitters is composed by a fraction Γ_S of gliotrasmitter-bounded receptors and a complementary $1 - \Gamma_S$ of available (not bounded) receptor, so that Γ_S evolves according to:

$$\frac{d\Gamma_S}{dt} = O_G G_A \, (1 - \Gamma_S) - \Omega_G \Gamma_S \tag{3}$$

Gliotrasmitter exocytosis

Astrocytic glutamate exocytosis is modeled akin to synaptic glutamate release, assuming that a fraction $x_A(t)$ of gliotransmitter resources is available for release at any time. Then, every time t_j that astrocytic Ca^{2+} increases beyond a threshold concentration C_θ, a fraction of readily releasable astrocytic glutamate resources, that is, $r_A(t_j) = U_A x_A(t_j^-)$, is released into the ECS and later reintegrated at rate Ω_A. Hence x_A evolves according to:

$$\frac{dx_A}{dt} = \Omega_A(1 - x_A) - \sum_j r_A \delta(t - t_j) \tag{4}$$

Similarly to synaptic case, it is possible to estimate the contribution to glutamate concentration in the ECS space (G_A), resulting from a quantal glutamate release event by the astrocyte at $t = t_j$, as $G_{rel}(t_j) = \rho_e G_T r_A(t_J)$, where G_T represents the total vesicular glutamate concentration in the astrocyte and ρ_e is the volume ratio between glutamate-containing astrocytic vesicles and periastrocytic space. Then, assuming a clearance rate of glutamate of Ω_e , the time course of astrocyte-derived glutamate in the ECS comprised between the astrocyte and the surrounding synaptic terminals is given by:

$$\frac{dG_A}{dt} = -\Omega_e G_A + \sum_j G_{rel} \delta(t - t_j) \tag{5}$$

Modulation of Synaptic Release by Gliostrasmitter

The gliotrasmitter modulation of synaptic release can be reproduce by the TM synaptic model, making the variable u_S in (1) depend on gliotrasmitter dynamics in the ECS, i.e. G_A in equation (5).
It may be assumed that basal synaptic release probability u_0 is not constant, but rather it is a function of G_A through the fraction Γ_S of presynaptic receptor that are activated by released gliotrasmitter molecules

$$u_0 \equiv u_0(G_A) = u_0(\Gamma_S(G_A)) \tag{6}$$

In the absence of quantitative physiological data, the function $u_0(\Gamma_S)$ can be taken analytic around zero that its firts-order expantion is considered accordingly:

$$u_0(\Gamma_S) \simeq u_0(0) + u_0'(0)\Gamma_S + O(\Gamma_S^2) \tag{7}$$

The zeroth-order term $u_0(0) = const = U_0^*$ corresponds to the value of u_0 in the absence of astocyte: that is the zeroth-order approximation fall back to the classic TM model (1). To express $u_0^{'}(0)$ instead, it may be noted that both $u_0(\Gamma_S)$ and Γ_S are defined in the interval [0, 1], so that $u_0(\Gamma_S)$ must either increase or decrease with Γ_S depending on whether gliotransmission stimulates or inhibits synaptic release. In the simplest scenario, the choice of $u_0^{'} = \alpha - U_0^*$ can be made so that, neglecting the terms of $O(\Gamma_S^2)$ in equations (7) ultimately provides

$$u_0(\Gamma_S) = U_0^* + (\alpha - U_0^*)\Gamma_S \tag{8}$$

The parameter α in the above equation lumps in a phenomenological way information on the effect of gliotransmission on synaptic release. For $0 \leq \alpha < U_0^*$, u_0 decreases with Γ_S, consistently with the *release-decreasing* effect of gliotrasmission on synaptic release. This could be the case of astrocytic glutamate targeting presyaptic kainate receptors or group II/III metabotropic receptors. For $U_0^* < \alpha \leq 1$, u_0 increase with Γ_S, consistent with a *release-increasing* effect of gliotrasmission on synaptic release, like in the case of glutamate in association with presynaptic NMDA receptors of group I metabotropic receptors. Finally, for $\alpha = U_0^*$, it is $u_0 = U_0^*$, independently of Γ_S. This case corresponds to *occlusion*, that is no net effect of gliotransmission on synaptic release due to the simultaneous activation of stimulatory and inhibitory receptors that may be co-expressed at the same synaptic terminal.

Synapse
$[u_S, x_S, Y_S, \Gamma_S]$

$$\dot{\Gamma_S} \equiv \dot{\Gamma_S}(G_A)$$
$$\dot{u_S} = -\Omega_f u_S$$
$$\dot{x_S} = \Omega_d(1 - x_S)$$
$$\dot{Y_S} = -\Omega_C Y_S$$

presynaptic Action Potential (AP)

$$u_0 = (1 - \Gamma_S)U_0^* + \alpha\Gamma_S$$
$$u_S \to u_S + u_0(1 - u_S)$$
$$r_S \to u_S x_S$$
$$x_S \to x_S - r_S$$
$$Y_S \to Y_S + \rho_S Y_T r_S$$

Astrocyte
$[I, h, C, \Gamma_A, x_A, G_A]$

$$\dot{\Gamma_A} \equiv \dot{\Gamma_A}(Y_S)$$
$$\dot{I} = J_\beta(\Gamma_A(Y_S)) + ...$$
$$\dot{C} = ...$$
$$\dot{h} = ...$$
$$\dot{x_A} = \Omega_A(1 - x_A)$$
$$\dot{G_A} = -\Omega_e G_A$$

Glio-Release Event - $C > C_\theta$ (GRE)

$$r_A \to U_A x_A$$
$$x_A \to x_A - r_A$$
$$G_A \to G_A + \rho_e G_T r_A$$

Figure 1: **Computational scheme of presynaptic pathway of gliotrasmitter modulation**. Synaptic variables with neurotrasmitter time course (red) and astrocytic variables with gliotrasmitter time course (green). The closed-loop gliotrasmission ensues from "cross dipendence" of G_A and Y_S. Mass balance equations for G-ChI model are reported in eqs (25) and (26).

In this study I want to go deeply into the analysis of presynaptic pathway of gliotrasmission concerning the glutamate, in particular the effect of release-decreasing on presynaptic release probability.

1.1 Modulation of synaptic release

How the presynaptic release probability r_S is modulated by release-decreasing gliotrasmission? The answer is set into equation (8), that explain how basal release probability changes in presence of astrocytic modulation.
Following the procedure presented in [4], I begin from the simplest situation: presynaptic neuron is a simple spikes generator, i.e. the spikes train is generated "by hand" and postsynapic neuron only monitors excitatory conductance g_e directly connected to excitatory synapses. The core is what happens in the synaptic cleft, in presence of relese-descresing effect.

In open-loop circuit, only the astrocyte influences the synaptic dynamics whereby the onset of calcium oscillations and the gliorelease depends only on endogenous IP_3 production. In Figure (2), indeed, the fraction of astrocytic binding with glutamate is always 0, while the I and C start to oscillate due to strong nonlinearity present in astrocytic dynamics (see equations (24), (25) and (26)).
The limit case of release-descreasing effect happens when α is equals to 0, in this case the time course of basal synaptic release (8) becomes:

$$u_0 = (1 - \Gamma_S)U_0^* \tag{9}$$

The dynamic behavior of Γ_S characterizes the neurotrasmitters release. After a gliorelease event (GRE) its value jumps into to range 0-1 and then falls back to zero as reported in Figure (3), thereby the released neurotrasmitter per action potential is generally lower than in the "simple" synapses - decreasing effect -. This amount, due to exponentially decay, tends to increase at every action potential with respect to preceding one, a phenomenon called facilitation.

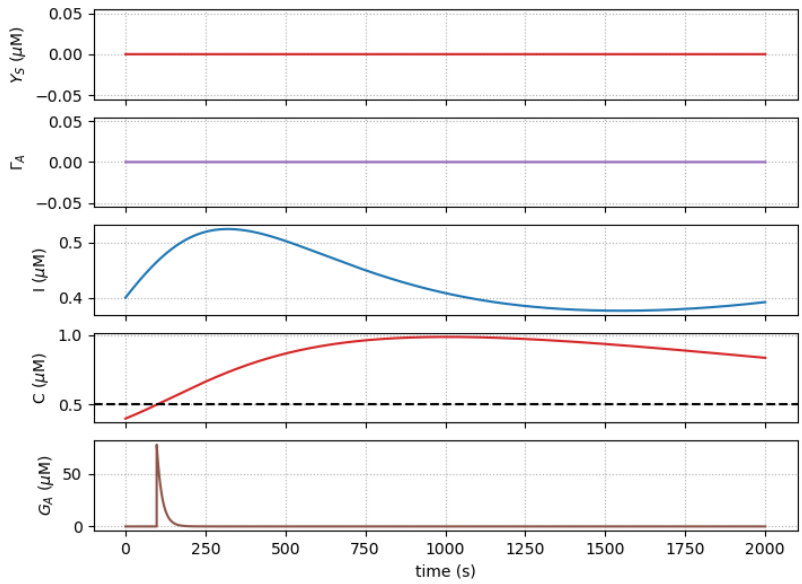

Figure 2: **Astrocytic variable dynamics in open-loop.** Astrocyte is not coupling with synapses whereby the fraction of binding receptor Γ_A is 0 (top panel) and the intracellular oscillations (I and C) depend on endogenous mechanisms. The gliorelease events is strongly releated with initial conditions of Ca^{2+} and IP_3 concentration: $I = 0.4$ and $C = 0.4$ lead to GRE at 97.55 ms (bottom panel), time simulation is 2 seconds.

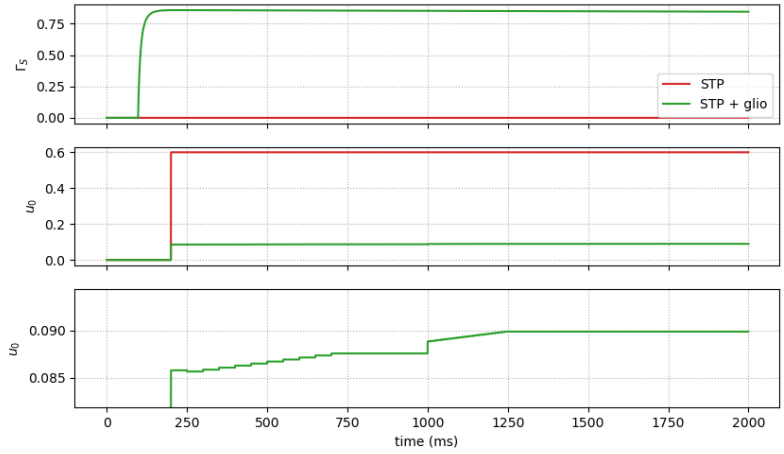

Figure 3: **Fraction of activated synaptic receptor and basal release probability in open-loop.** (top panel) Gliotrasmitter release at time 97.55 ms triggers an increase of Γ_S, (middle panel) the notable effects is the decreasing of basal release probability u_0 whose dynamics is connected with presynaptic action potential (bottom panel). The presynaptic spikes train is the same as in Figure (4).

Figure (4) illustrates how gliotrasmitter release could changes synaptic neurotrasmitter release in view of above consideration.

Presynaptic sample of spikes shows two different rate, 20 and 100 Hz. Without gliotrasmission the extracellular neurotrasmitter concentration Y_S progressively decreasing with the incoming action potentials (red traces), according to the depletion induced by STP. Taking into account gliorelease, indeed, leads

to *short-term facilitation*, that is a transient increase of neurotrasmitter release during consecutive APs (green traces).
Postsynaptic conductance g_e basically has the same behavior of Y_S, i.e. $g_e \rightarrow g_e + w_e\, r_S$, for this reason the facilitation is present in the same way.

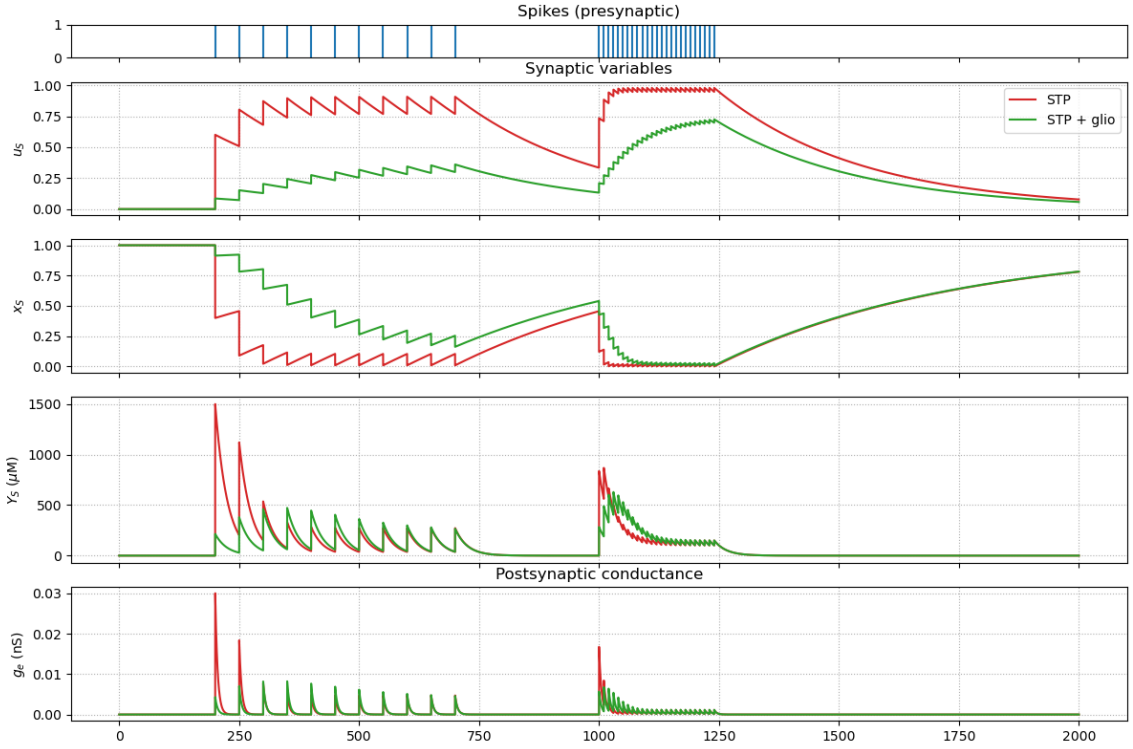

Figure 4: **STP facilitation in open-loop circuit.** (top panel) presynaptic sample of action potential, two different frequencies are present: 20 and 100 Hz. in both cases the facilitation effect is present, in particular with higher synaptic rate Y_S exceeds the correspondent values without gliotrasmission. GRE happens at 97.55 ms while first AP arrives at 200 ms.

The facilitation effect is profoundly affected by the fraction of activated synaptic receptor by gliotrasmitters Γ_S. It is plausible assume, looking equation (3), the concentration of gliotrasmitter G_A influences the neurotrasmitter release, i.e. r_S.
Figure (5) illustrates how the gliotrasmission effects change with respect to the concentration of gliotrasmitter released after a GRE (G_T). An increase of G_T leads to an increase of gliotrasmitter concentration in periastrocytic space G_A, thus the fraction on activated synaptic receptor increase, in other word the effect of gliotrasmission on synaptic release is stronger. As a consequence of stronger gliotrasmission, the basal release probability is brought close to 0 (top panel).
Short-term facilitation can be charaterized considering synaptic release due to pairs of APs, computing for each pair the paired-pulse ratio (PPR) of the fraction of neurotrasmitter released by the first AP.

$$\mathrm{PPR} = \frac{r_{S_{i+1}}}{r_{S_i}} \tag{10}$$

When PPR < 1 the neurotrasmitter released by the second AP is less than the amount released by the first AP (depression effect), coversely, if PPR > 1 the synaptic release increases with incoming of action potential (facilitation effect). Looking at the middle and the bottom panel in Figure (5) emerge these considerations:

- Without gliotrasmission (index 0) the depletion is dominant and the only "facilitation event" at 1000 ms depends on time evolution of synaptic variable, in this case we talk about recovery-from - depression (RFD).
- With gliotrasmission (indeces 1,2 and 3) short-term facilitation is strongly present and the transient time where it happens increase with G_T (index 1 has higher values of index 3).

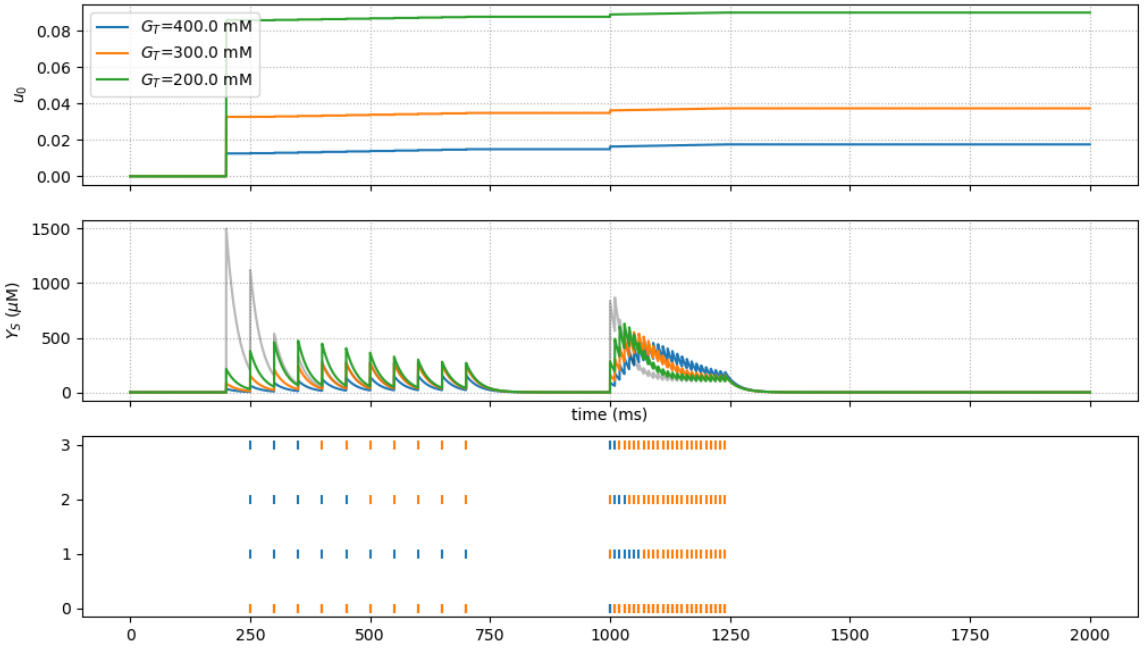

Figure 5: **STP facilitation with respect to G_T in open-loop circuit.** (Top panel) Increasing the gliotrasmitter release leas to an increase of Γ_S, as a consequence the basal release probability falls to 0. (middle panel) Neurotrasmitter relesed by consecutive APs shows differet behavior that can be quantified by PPR factor. (bottom panel) Every release event is colored in orange (depression) and in blue (facilitation), index 0 stand for the case without gliotrasmission while indeces 1, 2 and 3 are respectively the case of G_T = 400.0, 300.0 and 200.0 μM.

It is possible to consider a more realist situation with presynaptic spikes train come from Poisson distribution. Also in this situation, as reported in Figure (6), the facilitation effect is stronger for higher values of gliotrasmitter release from astrocyte.

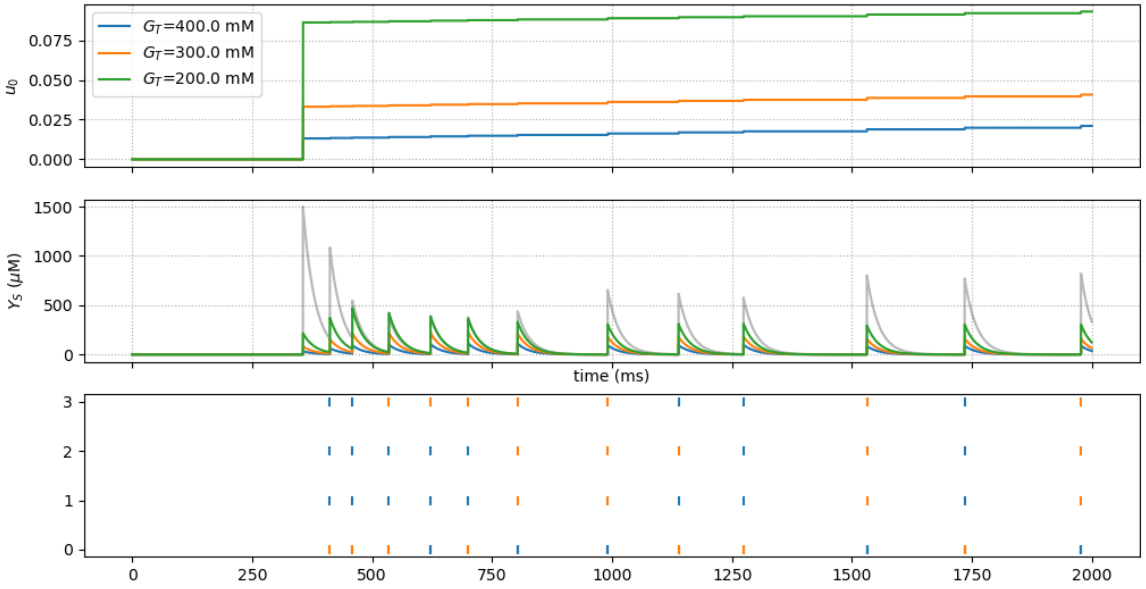

Figure 6: **STP facilitation with respect to G_T in open-loop circuit for Poisson presynaptic input.** The images are obtained with same condictios on Figure (5). A Poisson presynaptic spikes train with ν_{in}= 3.5 Hz substitutes the spikes train "by hand".

1.2 Closed- vs Open- Loop circuit

In previous discussion I only consider one-way interactions between synapse and astrocyte, the modulation of synaptic release by gliotrasmission. However in general case the other possible pathway, the modulation of gliotrasmission by synaptic release, may coexist with the other in so called closed-loop circuit.
The synaptic modulation triggers in astrocytes an addiction mechanism of IP_3 production depend on extracellular neurotrasmitters concentration (see Figure (1)). This exogenous IP_3 production changes the dynamics of I in the G-ChI model and, as a consequence, the Ca^{2+} oscillations.
Figure (7) describes the differences between open- and closed-loop scenario also in terms of gliorelease events (GRE). The main dynamic changes are found in the I time evolution (second panel), according to the onset of exogenous IP_3 production and, for the strong nonlinear coupling with C, also the timing of GREs are profoundly affected (bottom panel).

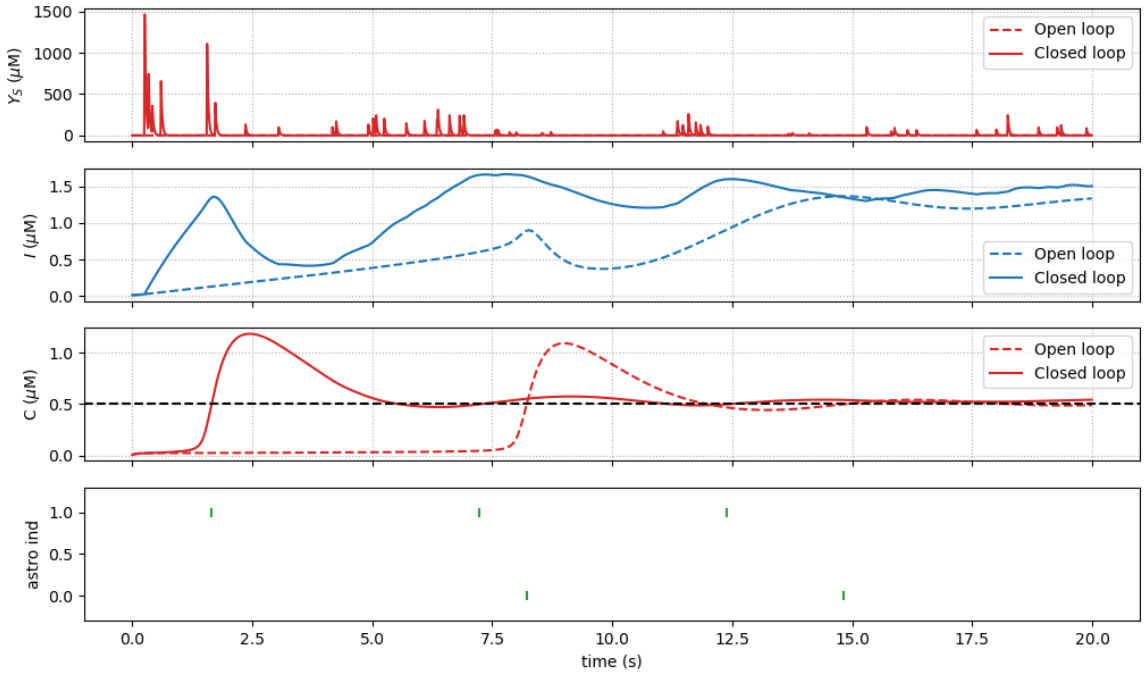

Figure 7: **Differences between astrocyte dynamics in open- and close- loop**. Astrocytes variable dynamics in open- (dashed) and closed-loop (solid) circuit. Exogenous IP_3 production deeply changes the I time evolution and this is reflected in the GREs time distribution (bottom panel, 0 = open, 1 = closed). Initial conditions: I=C=0.01 μM, h=0.9, Y_S=0 μM

To elucidate some of possible functional implications of closed-loop gliotrasmission, the average synaptic release for N_{syn}=160 identical synapses is computed for costant stumulus and compare it to the open-loop scenario as well as simple synapses without gliotrasmission.

Figure (8) shows some simulations of gliotransmission for time evolution of average neurotrasmitter concentration in the synaptic cleft in response to constant input rate[1]. Gliotrasmission dramatically changes the synaptic transmission.
The facilitation effect is visible both for open and closed circuit, after a gliorelease event the neurotrasmitter abruptly decrease (at 2 s, 8 s and 14 s for closed-loop and at 8 s and 15 s for open-loop) and then increasing according to facilitation effect. The notable differences are found in GRE distribution shows in right panel: while the astrocytes in open-loop fire at the same time, in closed-loop this distrubution of GREs are sparse.

[1]Authors in [4] studied the responses to a steps funcion of incoming action potential to describe also the behavior or gliotrasmission when the input changes during time simulation. Here I put myself in a simple situation

Also in this situation, Γ_S is the main protagonist of time evolution and, in particular, of the onset of facilitation effect.
In figure (9) there are different time courses with respect to Ω_G, agonist release (deactivating) rate (see equations (3)). An increase of Ω_G changes the exponential decay rate of Γ_S, such that both open and closed faster approximate the no gliotrasmission case, i.e. Γ_S equals to O (top rows in Figure (9)). This is clearly visibile in the Y_S time evolution, with high Ω_G its values is very similar to no gliotrasmission one. In principle might be exist a dependence with respect to G_T, but these simulations does not this behavior (data not shown).

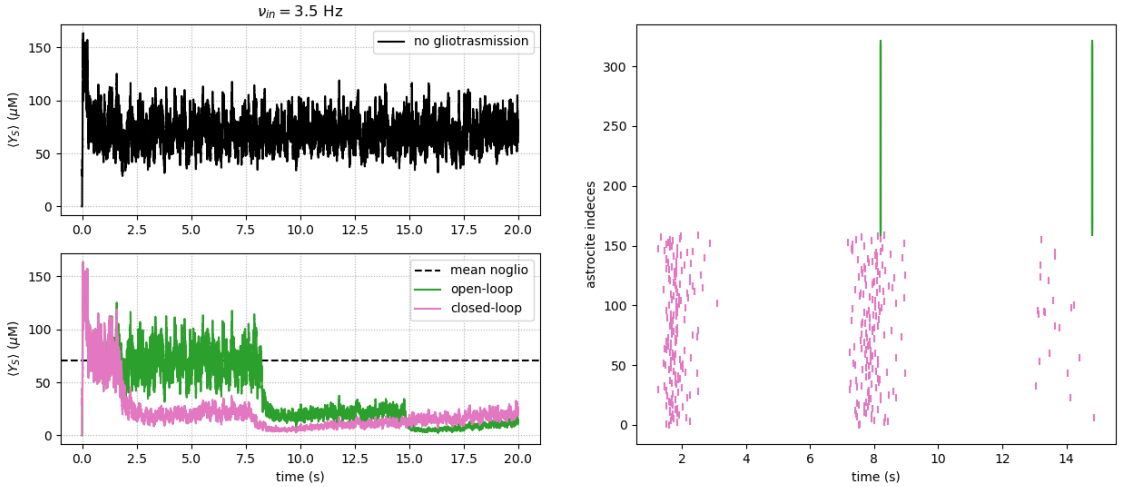

Figure 8: **Average neurotrasmitter release in case of no gliotrasmission, open- and closed-loop**. (left panels) Average neurotrasmitter release on 160 indipendent identical synapses for 20 seconds long simulation, presynaptic firing rate is 3.5 Hz. (right panel) Raster plot of GRE, astrocytes labeled from 0 to 160 (pink marker) are part of closed-loop, the other one (green) of open-loop. Initial conditions: I=C=0.01 μM, h=0, Y_S=0 μM

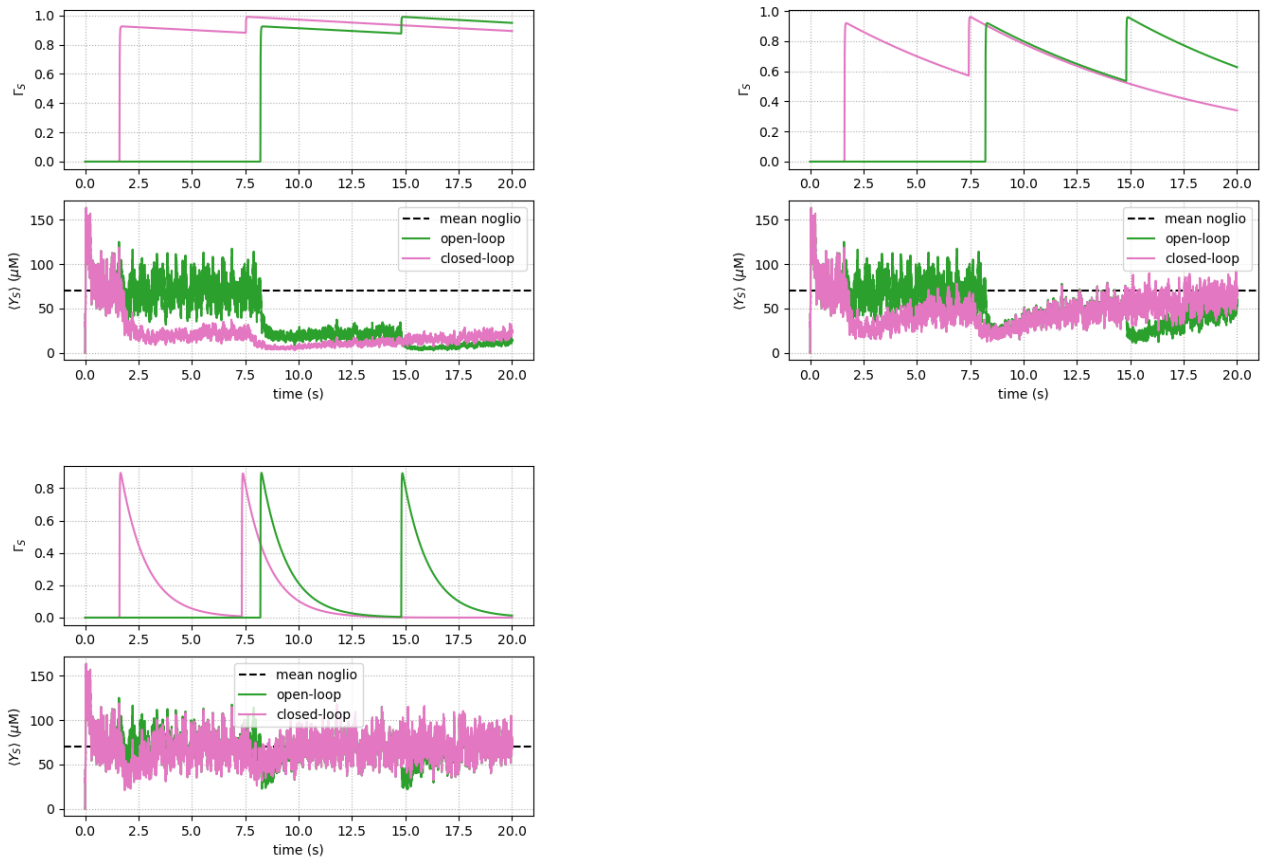

Figure 9: **Gliorelease effect with respct to** Ω_G. Average neurotrasmitter release on 160 indipendent identical synapses for 20 seconds long simulation. (top left) $\Omega_G = 0.0083$ Hz; (top right) $\Omega_G = 0.0833$ Hz; (bottom left) $\Omega_G = 0.8333$ Hz.

The differences in terms of modulation effects between open- and closed-loop are further elucidated looking at the average synaptic release for different rates of randomly incoming action potentials. In this way it may be possible to analyse the nature of filtering behavior in presence of gliotrasmitters release.

The low-pass filter characteristics of synapses without gliotrasmission is visible in top left panel in Figure (10), with low presynaptic firing rate the inter-spikes interval (ISI) are big enough to allow the restoring of synaptic resources, the average of r_S perhaps is equal to 0.6 namely the value in absence of plasticity. For higher firing rate, instead, the synaptic depletion leads to decrease r_S.
In closed-loop circuit, the nature of filtering characteristics changes into a band-pass filter (bottom left in Figure (10)). A qualitative explanation may be found into the combination of release-decreasing and facilitation effects: [2]

- low presynaptic rates (less than 0.8 Hz). As the no gliotrasmission situation, the inter-spikes interval is big enough to allow the recovering of synaptic resources. In addiction the low synaptic activity makes the astrocytic variables in a range close to gliorelease threshold (left column in Figure (12)), thus the gliorelease events are relative close to each others as shown in raster plot in Figure (10). The consequences is, according to the previous discussions, Γ_S lies in a range close to 1, thus for equation (9) basal release probability is strongly close to 0 due to release-decreasing effect. In conclusion the mean of r_S is lower than no gliotrasmission scenario.

- middle presynaptic rates (from 0.8 Hz to 3.5 Hz). Increasing the presynaptic firing rate leads to increase both neurotrasmitter concentration into the synaptic cleft and the antagonist binding-receptor

[2] Authors in [4] studied more general systems. To tacking into account the possible interaction between two astrocytes, a further term of exogenous IP_3 production is added into equation (24) stands for the possible IP_3 diffusion through gap junction. Their filtering characteristics are slightly differnt from the simple situation where astrocyte-to-astrocyte connections are neglected.

of astrocyte. The exogenous production of IP_3 is stronger than low presynaptic input rates, thus the steady state of I and C are higher (middle column in Figure (12)). The notable consequence is that the time between two consecutive gliotrasmitter release are big enough to allow Γ_S to decrease. For this the facilitation effect is triggered and r_S increses.

- high presynaptic rates (greater than 10 Hz). For high input rates the synapses cannot sustain further gliotrasmission release (right column in Figure (12)), thus the synaptic transmission becomes independent of gliotrasmission as if it were in simple scenario without gliotrasmission.

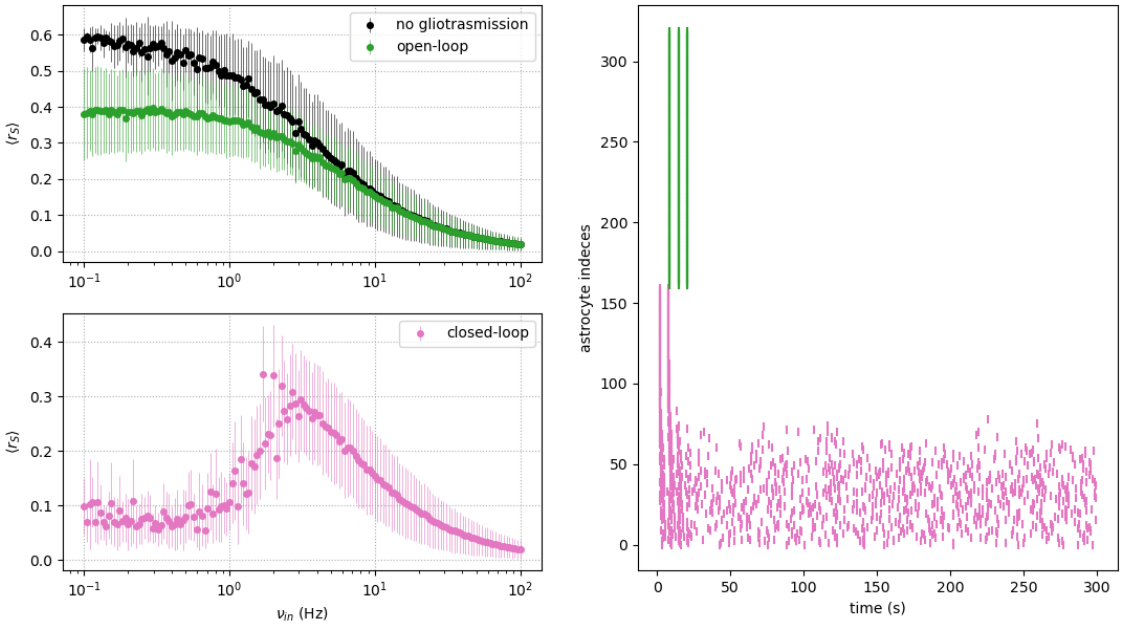

Figure 10: **Average release probability for different incoming action potential**. Average of r_S of 160 independent synapses for the three different situation, time simulation covers 300 second for each synapse but only the data after 50 seconds are taken to evaluate mean and standard deviation, integration steps is 1 ms. (top left) No gliotrasmission and open-loop situation, there are no differences of filtering behavior. (bottom left) The lwo-pass filter becomes a band-pass filter in closed-loop circuit due to the combination of release-decreasing and facilitation effects. (right panel) GREs raster plot about open (green) and closed (pink) situation.

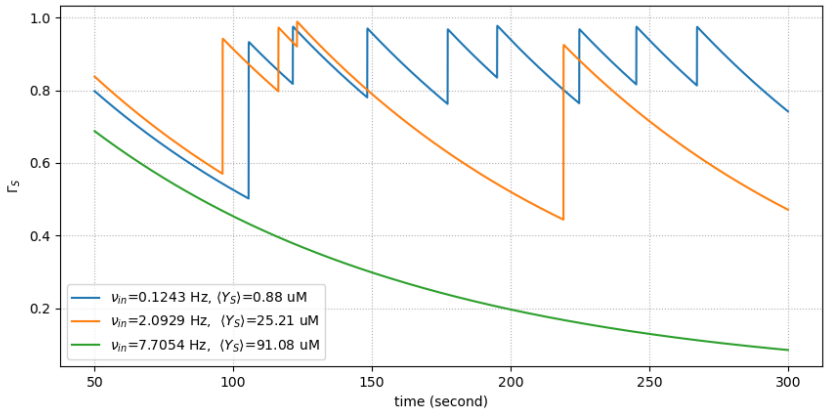

Figure 11: **Time evolution of synaptic variable in r_S modulation**. Time evolution Γ_S is intimate related to the onset of facilitation, the combination of its time course and the incoming action potential rates define the filtering behavior. Input rate: 0.12 (blue), 2.09 (orange) and 7.7 Hz (green)

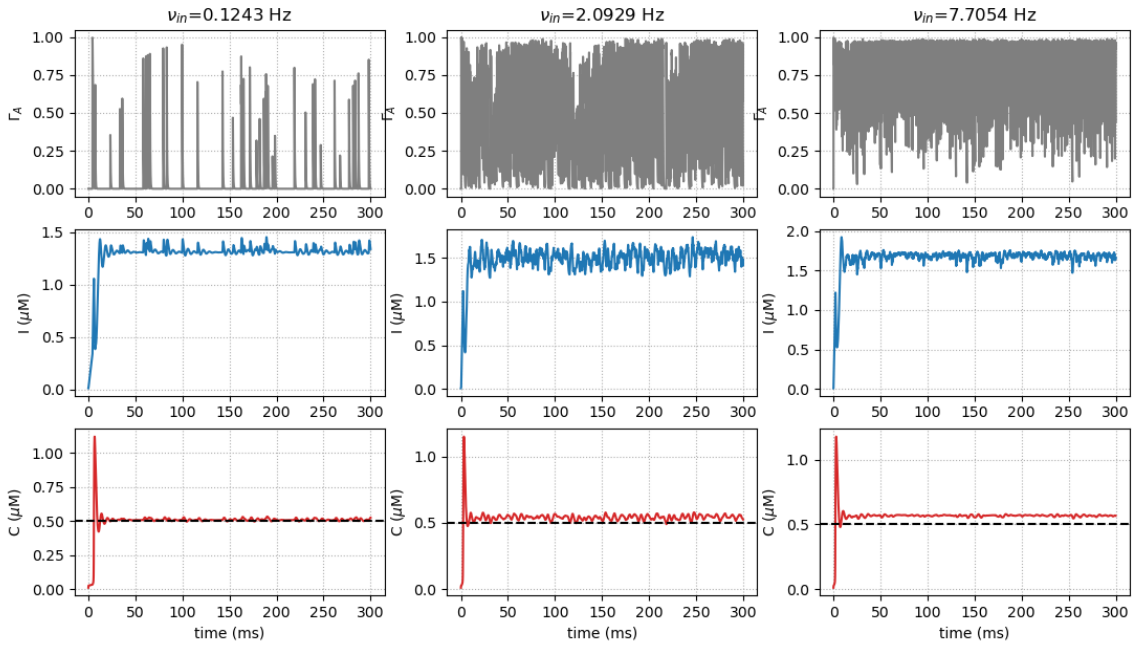

Figure 12: **Astrocyte dynamics with three different incoming action potential rates**.

1.3 Local circuit of the Network

In conclusion, to better understand the functional implication of gliotrasmisson and the effects that could have into the excitatory inhibitory neuronal network, I have studied the time evolution of postsynaptic neuron connected with 160 presynaptic excitatory inputs.
The goal is to compute the postsynaptic conductance g_e without gliotrasmission and in presence of closed loop and compare their with results pf previous section. In addiction it is possible to compute also the average neurotrasmitter release from the g_e data using the follow equations:

$$\begin{aligned} \overline{\Delta g_e} &= \frac{1}{N_{tot}} \sum_{K,k} w_e \, r_S(t_k^K) \\ \overline{r_{S_{exc}}} &= \frac{\overline{\Delta g_e}}{w_e} \end{aligned} \tag{11}$$

where t_k^K is the k-th spike timing of excitatory presynaptic neuron K. From this data it is possible to have another prove of filtering behavior of synapses in realistic situation.

The presynaptic spikes train comes from 160 identical synapses fire in Poisson fashion with identical input rate. The data about the average neurotrasmitters release are computed through (11) over a total time simulation of 250 seconds but the mean are computed only after 5 seconds. The results of $\overline{r_{S_{exc}}}$ are collected in the fallowing table:

ν_{in} (Hz)	$\overline{r_{S_{exc}}}$ **no gliotrasmission**	**closed-loop**
0.12	0.58	0.08
2.09	0.43	0.26
3.00	0.39	0.29
7.70	0.29	0.25
30.00	0.20	0.18
100.00	0.12	0.11

Table 1: $\overline{r_{S_{exc}}}$ for 250 seconds long time simulation with 5 seconds transient time

Even if the low amount of data it is clear that the filtering characteristics are preserved. Without gliotrasmission, indeed, the neurotrasmitters release decreases while, in closed-loop this values reaches a maximum at 3.00 Hz according to results shown in Figure (10). Neverthless it is important to underling that this filtering features, at least for this particular set of parameters, emerge for long observation (simulation) time, that is the time windows where we can appreciate the facilitation effects. If the data are recorded only for 50 seconds or less, Γ_S has not enough time to restore itself and the facilitation is strongly attenuated (see Figure (13)), and this attenuation provides an underestimation of neuritrasmitter release. Accordingly, $\overline{r_{S_{exc}}}$, for 50 seconds long simulation time and without transient, assumes the values in Table (2):

ν_{in} (Hz)	$\overline{r_{S_{exc}}}$ **no gliotrasmission**	**closed-loop**
0.12	0.58	0.10
2.09	0.40	0.11
3.00	0.35	0.12
7.70	0.21	0.12
30.00	0.10	0.07
100.00	0.05	0.04

Table 2: $\overline{r_{S_{exc}}}$ for 50 secodns long time simulation without transient time

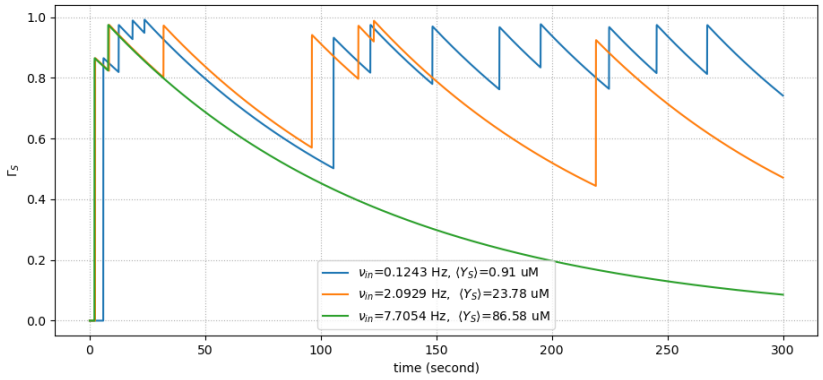

Figure 13: **Time evolution of synaptic variable in r_S modulation, no transient time**. Same plots as in Figure (11) without transient time. Because of the characteristic time constant of Γ_S, during the first 50 seconds the facilitation effects is strongly attenuated.

Last open question concern how the postsynaptic excitatory conductance is modulated by gliotrasmission. The aswer of this question is found into the combination of all above conclusion, Figure (14) summarises all the concepts that are elucidated before and helps us to get some notable insights about the neuro-glia interactions at network level.

Postsynaptic conductance g_e has got the same dynamics of Y_S, a exponential clearance combined with a steps increase at action potential arrival. For this reason release decreasing effect and short-term facilitation are both present as reported in Figure (8).
In presence of gliotrasmission the value of g_e is always lower then in simple synapses (respectively pink and black traces in left column in Figure (14)) but, especially when ν_{in} is close to the maximum of bell-shape curve (middle row), tends to recovery the value fixed by simple scenario, according to the facilitation effects.

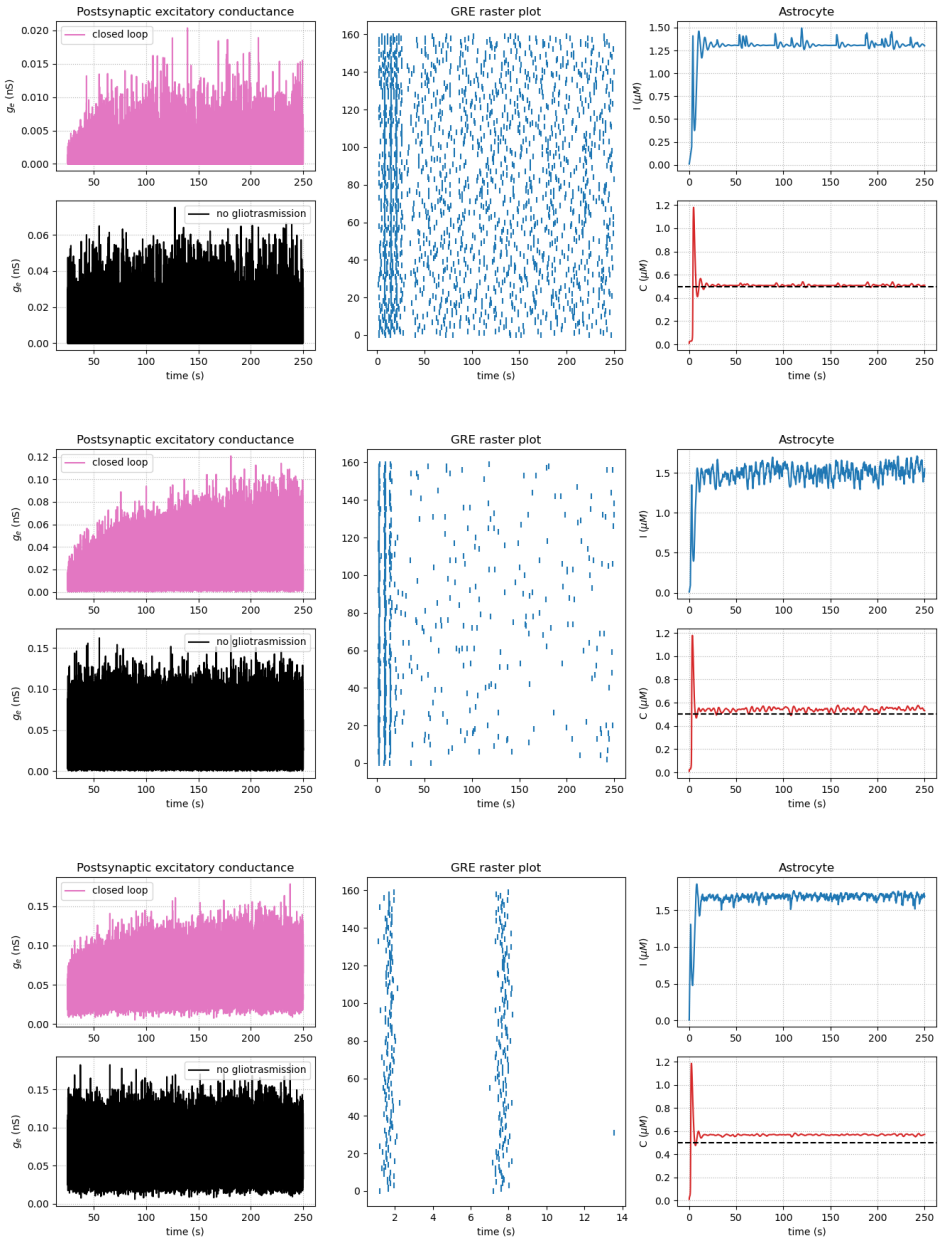

Figure 14: **Postsynaptic excitatory conductance dynamics with respect three different input rate**. Postsynaptic neurons, both in no gliotrasmission and closed loop circuit are connected with 160 presynaptic (excitatory) synapses each of them fire with equal rate. The simulations run for 250 seconds (integration step is 0.5 ms)for each value of input rate: 0.12 Hz(top), 2.09 Hz (middle) and 7.70 Hz (bottom). The g_e in gliotrasmission modulation (pink traces) are alway lower than in simple synapses (black traces) according to relese-descresing effect, furthermore in the first case the value tends to increase (facilitation effects) in time "trying to reach" the maximum value fixed by simple scenario. GRE raster plots and the dynamics of astrocyte variable are equals to above discussion.

All the considerations emerged (if correct) in this report could be useful to set the right computational setting of neuron-glia network. First of all, with constant external input rate, the total time simulation

might be long enough to appreciate the short-term facilitation, namely at least 100 seconds with transient time of 20-30 seconds to avoid the bias introduced by initial conditions. In addiction, the increasing in time of postsynaptic conductance might give an notable insight about how the modulation induced by astrocytes could be restored the balance between excitatory and inhibitory recurrent inputs during the network dynamics.

1.4 Mean field derivation of dynamical synapses

The phenomenological models of dynamical synapses can be used to analyse the way activity of large population of presynaptic neurons is transmitted to postsynaptic target. The model equations in (1) can be manipulated to derived a mean field description of synaptic dynamics, and thus of short-term plasticity. Furthermore the following methods could be generalized to derive an approximation also in presence of gliotrasmission (see reference [5]).

The equation of dynamical synapses could be seen composed by two part: the time evolution between two consecutive spikes and what happens upon arrival of a generic spike. For instance before the first spike, i.e. $[t_0, t_1)$, the synaptic variable evolves according to:

$$\begin{aligned} \frac{du_S}{dt} &= -\Omega_f u_S \\ \frac{dx_S}{dt} &= \Omega_d(1 - x_S) \end{aligned} \tag{12}$$

This equations describe the time course of synaptic variable at the same time before the spikes, with this regards the variable could be replaced by u_S^- and x_S^-. The spikes arrival triggers the increase of release probability and the release of neurotrasmitter resources, thus at time t_1:

$$\begin{aligned} u_S^+ &= u_S^- + u_0(1 - u_S^-) \\ r_S(t_1) &= u_S^+ \, x_S^- \\ x_S^+ &= x_S^- - u_S^+ \, x_S^- \end{aligned} \tag{13}$$

To generalize the above consideration, the dynamics with generic spikes train is completely described by the following set of equations:

$$\begin{aligned} \frac{du_S^-}{dt} &= -\Omega_f u_S^- + u_0 \sum_k (1 - u_S^-)\delta(t - t_k) \\ \frac{dx_S^-}{dt} &= \Omega_d(1 - x_S^-) - \sum_k u_S^+ \, x_S^- \delta(t - t_k) \\ u_S^+ &= u_S^- + u_0(1 - u_S^-) \end{aligned} \tag{14}$$

Equations (14) is a nonlinear system of two ODEs, substituting the third expression into the first one provides:

$$\begin{aligned} \frac{du_S^+}{dt} &= \Omega_f(u_0 + u_S^+) + u_0 \sum_k (1 - u_S^+)\delta(t - t_k) \\ \frac{dx_S^-}{dt} &= \Omega_d(1 - x_S^-) - \sum_k u_S^+ \, x_S^- \delta(t - t_k) \end{aligned} \tag{15}$$

To simplify the notation, I following redefine the variable without the + and - apexes.
Consider then n_S trials of stimulation of a synapse by trains of APs of equal length and same statistics, delivered to the synapse at identical initial conditions. The trial-averaged synaptic dynamics for the mean AP is described by equations (15) in term of mean quantities $\bar{u_S} = 1/n_S \sum_l^{n_s} u_{S_l}$ and $\bar{x_S} = 1/n_S \sum_l^{n_s} x_{S_l}$,

$$\begin{aligned} \frac{d\bar{u_S}}{dt} &= \Omega_f(u_0 + \bar{u_S}) + \frac{u_0}{n_S} \sum_l^{n_S} \sum_k (1 - u_{S_l}) \, \delta(t_{k_l}) \\ \frac{d\bar{x_S}}{dt} &= \Omega_d(1 - \bar{x_S}) - \frac{1}{n_S} \sum_l^{n_S} \sum_k u_{S_l} x_{S_l} \, \delta(t_{k_l}) \end{aligned} \tag{16}$$

In a small time interval Δt, the above equations can be rewritten in terms of finite differences as:

$$\begin{aligned} \bar{u_S}(t+\Delta t) - \bar{u_S}(t) &= \Omega_f(u_0 + \bar{u_S})\Delta t + \frac{u_0}{n_S}\sum_l^{n_S}(1-u_{S_l})\,\Delta_l(\Delta t) \\ \bar{x_S}(t+\Delta t) - \bar{x_S}(t) &= \Omega_d(1-\bar{x_S})\Delta t - \frac{1}{n_S}\sum_l^{n_S} u_{S_l}x_{S_l}\,\Delta_l(\Delta t) \end{aligned} \tag{17}$$

where $\Delta_l(\Delta t) = \sum_k \delta(t - t_{l_k})\Delta t$ is the number of spikes in the time interval Δt for the lth trial and is a strongly stochastic quantity.
Analysis of neurophysiological data revealed that individual neurons in vivo fire irregularly at all rates, reminiscent of a Poisson process. Mathematically, the Poisson assumption means that, at each moment, the probability that a neuron fires equals the neuron's instantaneous firing rate and is independent of the timing of previous APs. Then, assuming that the n_S trains of APs under consideration are different realizations of the same Poisson process with average rate $\nu_S(t)$, equations (17) can be averaged in time over a proper Δt. In particular, thanks to the Poisson hypothesis, the variable u_S, x_S, $u_S x_S$ and $\Delta_l(\Delta t)$ can be consider independent and thus be averaged independently.
Therefore, taking Δt of a order of several intervals between spikes, but shorter than longest time scale in the system ($1/\Omega_d$ and $1/\Omega_f$), the time average (denoted by $\langle x\rangle$) of $\Delta_l(\Delta t)$ can be estimate by $\Delta_l(\Delta t) = \nu_S(t)\Delta t$. Accordingly,

$$\begin{aligned} \langle\bar{u_S}(t+\Delta t)\rangle - \langle\bar{u_S}(t)\rangle &= \Omega_f(u_0 + \langle\bar{u_S}\rangle)\Delta t + \frac{u_0}{n_S}\sum_l^{n_S}(1-\langle u_{S_l}\rangle)\,\nu_S(t)\Delta t \\ \langle\bar{x_S}(t+\Delta t)\rangle - \langle\bar{x_S}(t)\rangle &= \Omega_d(1-\langle\bar{x_S}\rangle) - \frac{1}{n_S}\sum_l^{n_S}\langle u_{S_l}x_{S_l}\rangle\,\nu_S(t)\Delta t \end{aligned} \tag{18}$$

Finally, divided by Δt yields

$$\begin{aligned} \frac{d\langle\bar{u_S}\rangle}{dt} &= \Omega_f(u_0 + \langle\bar{u_S}\rangle) + u_0(1-\langle\bar{u_S}\rangle)\,\nu_S(t) \\ \frac{d\langle\bar{x_S}\rangle}{dt} &= \Omega_d(1-\langle\bar{x_S}\rangle) - \langle\bar{u_S}\rangle\langle\bar{x_S}\rangle\,\nu_S(t) \end{aligned} \tag{19}$$

that is a nonlinear and nonautonomous set of two ODEs and describe the dynamics of average synaptic variables. In general it is possible to resolve analytically the first equations and then, putting the results in the second, resolve the whole system. However, when the presynaptic firing rate is constant in time, i.e. $\nu_S(t) = \nu_S$, the system becomes autonomous and it is possible to evaluate the steady states. Accordingly, the intersection of nunclines provides the fixed points for the systems:

$$\begin{aligned} \langle\bar{u_S}\rangle &= \frac{u_0(\Omega_f + \nu_S)}{\Omega_f + \nu_S\,u_0} \\ \langle\bar{x_S}\rangle &= \frac{\Omega_d}{\Omega_d + \langle\bar{u_S}\rangle\,\nu_S} \end{aligned} \tag{20}$$

Now it is easy to estimate the behavior with extreme values of presynaptic firing rate. In presence of low firing rate, i.e. $\nu_S \to 0$, the probability of release tends to $u_0 = 0.6$ and the available neurotrasmitter resorses tends to 1, thus the $r_S = u_S x_S \to u_0$. Conversely for high firing rate, i.e. $\nu_S \to +\infty$, u_S tends to 1 and x_S tends to 0, therefore the average values of neurotrasmitter is 0.
This conclusion are in totally agreement with the qualitative discussion about the filtering behavior of simple synapse. In addiction, the approximate solution of $r_S = u_S x_S$ shown in Figure (15) is similar to numerical solution presented in Figure (10).

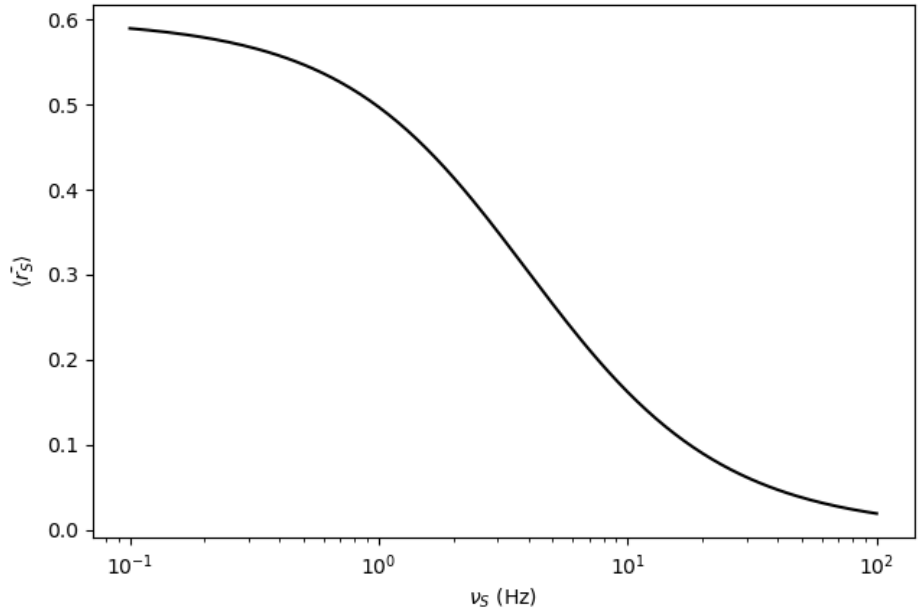

Figure 15: **Mean field approximation solution of released neurotrasmitter in simple synapses**. Approximation solution of average value of r_S.

Questions about Mean field

The author in [3] writes down a similar set of equations describing the dynamical synapses:

$$\begin{aligned} \frac{du_S^+}{dt} &= -\Omega_f u_S^+ + u_0 \sum_k (1 - u_S^+)\delta(t - t_k) \\ \frac{dx_S^-}{dt} &= \Omega_d (1 - x_S^-) - \sum_k u_S^+ x_S^- \delta(t - t_k) \\ u_S^- &= u_S^+ + u_0(1 - u_S^+) \end{aligned} \tag{21}$$

The differences are in the first and in the last equations where u_S^- in (14) becomes u_S^+. Then, substituting u_S^+ into the first equations the final set is equals to (16) and the conclusion is the same. I don't understand the mathematics beyond this kind of procedure.

- Equations in (21) provide the following relation between u_S just before and after a spikes:

$$u_S^+ = \frac{u_S^- - u_0}{1 - u_0} \tag{22}$$

  At very beginning, when u_S^- is 0, this leads to a negative values for u_S^+ and this is impossible because the probability is in range 0 and 1.

Appendix A G-ChI astrocyte model

A corollary of the biological and modeling arguments is that Ca^{2+} and IP_3 signals are, generally speaking, dynamically coupled in astrocytes.
A model that deals with this coupling is the so-called ChI which is constituted by three ODEs, respectively, for intracellular Ca^{2+} (C), the IP_3R gating variable h, and the mass balance equation for intracellular IP_3 lumping terms:

$$\begin{aligned}\frac{dC}{dt} &= J_r(C,h,I) + J_l(C) - J_p(C)\\ \frac{dh}{dt} &= \frac{h_\infty(C,I) - h}{\tau_h(C,I)}\\ \frac{dI}{dt} &= J_\delta(C,I) - J_{3K}(C,I) - J_{5P}(I)\end{aligned} \tag{23}$$

The above model can also be extended to include GPCR dynamics by the G-ChI model. To this aim, the contribution of GPCR-mediated IP_3 synthesis is added to the right-head side of (23):

$$\begin{aligned}\frac{d\Gamma_A}{dt} &= O_N Y_S(1-\Gamma_A) - \Omega_N\left(1+\zeta\mathcal{H}_1(C,K_{KC})\right)\Gamma_A\\ \frac{dC}{dt} &= J_r(C.h,I) + J_l(C) - J_p(C)\\ \frac{dh}{dt} &= \frac{h_\infty(C,I) - h}{\tau_h(C,I)}\\ \frac{dI}{dt} &= J_\beta(\Gamma_A) + J_\delta(C,I) - J_{3K}(C,I) - J_{5P}(I)\end{aligned} \tag{24}$$

where Y_S stands for the neurotrasmitter concentration in the periastrocytic space. The mass balance equation for C is described by:

$$\begin{aligned}J_p(C) &= O_P\mathcal{H}_2(C,K_P)\\ J_l(C) &= \Omega_L(C_T - (1+\rho_A)C)\\ J_r(C,h,I) &= \Omega_C m_\infty^3 h_\infty^3(C_T - (1+\rho_A)C)\end{aligned} \tag{25}$$

Similary for IP_3 dynamics:

$$\begin{aligned}J_\beta &= O_\beta\Gamma_A\\ J_\delta &= \Omega_L(C_T - (1+\rho_A)C)\\ J_{3K} &= O_{3K}\mathcal{H}_4(C,K_D)\mathcal{H}_1(I,K_3)\\ J_{5P} &= \Omega_{5P}I\\ J_\delta &= O_\delta\frac{\kappa_\delta}{\kappa_\delta + I}\mathcal{H}_2(C,K_\delta)\end{aligned} \tag{26}$$

Starting from model (24) it is possible to analyse the dynamical feature of astrocytes.
The above results suggests intracellular calcium concentration deeply influences the filtering features of tripartite synapses. An astrocyte defined by parameters in B.2 show a stable fixed points for a wide range of Y_S values, notably the steady states are always beyond threshold (Figure (16)).

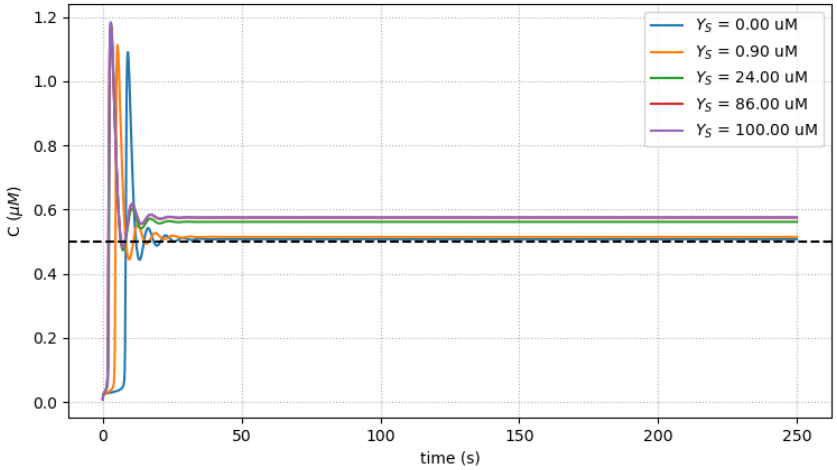

Figure 16: **Astrocyte steady state with respect to extracellular neurotrasmitter concentration** . Calcium steady states with 5 different Y_S values. Simulation runs for 250 seconds with 0.01 seconds of integration time step.

The system goes into the steady state through an initial transient regime where the oscillations depends on initial conditions. Thus, after 50 second, the only possibility for gliotrasmitter release is a change of Y_S.

Appendix B Model Parameters used in the simulations

The following tables report constants that corresponds to the model parameters used in the simulation.

B.1 Neurons and synapses

Symbol	Name in code	Value	Units	Description
		Neuron parameters		
C_m	`C_m`	198	pF	Membrane capacitance
E_l	`E_l`	-60	mV	Leak reversal potential
g_l	`g_l`	9.99	nS	Leak conductance
V_r	`V_r`	-60	mV	Reset potential
V_θ	`V_th`	-50	mV	Firing threshold
τ_r	`tau_r`	5	ms	Refractory period
		Synapse parameters		
Ω_d	`Omega_d`	2	s^{-1}	Synaptic depression rate
Ω_f	`Omega_f`	3.33	s^{-1}	Synaptic facilitation rate
U_0^*	`U_0__star`	0.6	-	Resting synaptic release probability
Y_T	`Y_T`	500	mM	Total vesicular neurotramitter concentration
ρ_c	`rho_c`	0.005	-	Synaptic vesicle-to-extracellular space volume ratio
Ω_c	`Omega_c`	40	s^{-1}	Neurotrasmitter clearance rate
w_e	`w_e`	50	pS	Excitatory synaptic conductance
w_i	`w_i`	1	nS	Inhibitory synaptic conductance
τ_e	`tau_e`	5	ms	Excitatory synaptic time constant
τ_i	`tau_i`	10	ms	Inhibitory synaptic time constant
E_e	`E_e`	0	mV	Excitatory synaptic reversal potential
E_i	`E_i`	-80	mV	Inhibitory synaptic reversal potential
		Presynaptic receptor parameters		
O_G	`O_G`	1.5	μM s-1	Agonist binding (activating) rate
Ω_G	`Omega_G`	0.5	min^{-1}	Agonist release (deactivating) rate

B.2 Astrocyte

Symbol	Name in code	Value	Units	Description
		Ca^{2+}-induced Ca^{2+} release		
C_T	C_T	2	μM	Total cell free Ca^{2+} content
ρ_A	rho_A	0.18	-	ER-to-cytoplasm volume ratio
d_1	d_1	0.13	μM	IP_3 binding affinity
d_2	d_2	1.05	μM	Ca^{2+} inactivation dissociation constant
d_3	d_3	0.9434	μM	IP_3 dissociation constant
d_5	d_5	0.08	μM	Ca^{2+} activation dissociation constant
O_2	O_2	0.2	μM s^{-1}	IP_3R binding rate for Ca^{2+} inhibition
Ω_C	Omega_C	6	s^{-1}	Maximal rate of Ca^{2+} release by IP_3Rs
Ω_L	Omega_L	0.1	s^{-1}	Maximal rate of Ca^{2+} leak from the ER
O_P	O_P	0.9	μM s^{-1}	Maximal Ca^{2+} uptake rate by SERCAs
K_P	K_P	0.05	μM	Ca^{2+} affinity of SERCAs
		IP_3 signaling		
O_β	O_beta	0.5	μM s^{-1}	Maximal rate of IP_3 production by PLCβ
O_δ	O_delta	1.2	μM s^{-1}	Maximal rate of IP_3 production by PLCδ
κ_δ	kapppa_delta	1.5	μM	Inhibition constant of PLCδ by IP_3
K_δ	K_delta	0.1	μM	Ca^{2+} affinity of PLCδ
O_{3K}	O_3K	4.5	μM s^{-1}	Maximum rate of IP_3 degradation by IP_3-3K
K_{3K}	K_3K	1.0	μM	IP_3 affinity of IP_3-3K
K_D	K_D	0.7	μM	Ca^{2+} affinity of IP_3-3K
Ω_{5P}	Omega_5P	0.05	s^{-1}	Maximal rate of IP_3 degradation by IP-5P
		Metabotrobic receptor kinetics		
O_N	O_N	0.3	μM s^{-1}	Agonist binding rate
Ω_N	Omega_N	0.5	s^{-1}	Maximal inactivation rate
K_{KC}	K_KC	0.5	μM	Ca^{2+} affinity of PKC
ζ	zeta	10	-	Maximal reduction of receptor affinity by PKC
		Gliotrasmission		
C_θ	C_theta	0.5	μM	Ca^{2+} threshold for exocytosis
G_T	G_T	200	mM	Total vesicular gliotrasmitter concentration
Ω_A	Omega_A	0.6	s^{-1}	Gliotrasmitter recycling rate
U_A	U_A	0.6	-	Gliotrasmitter release probability
ρ_e	rho_e	6.5 10^{-4}	-	Astrocitic vesicle-to-extracellular volume ratio
Ω_e	Omega_e	60	s^{-1}	Gliotrasmitter clearence rate
α	alpha	0	-	Gliotrasmission nature

References

[1] De Pittà, M.D., Ben-Jacob, E., Berry, H. (2019). G Protein-Coupled Receptor-Mediated Calcium Signaling in Astrocytes. Springer Series in Computational Neuroscience.

[2] González-Arias C., Perea G. (2019). Gliotransmission at Tripartite Synapses. In: De Pittà M., Berry H. (eds) Computational Glioscience. Springer Series in Computational Neuroscience. Springer, Cham.

[3] De Pittà M. (2019). Gliotrasmission Exocytosis and Its Consequences on Synaptic Transmission. In: De Pittà M., Berry H. (eds) Computational Glioscience. Springer Series in Computational Neuroscience. Springer, Cham.

[4] Stimberg M., Goodman D.F.M., Brette R., Pittà M.D. (2019) Modeling Neuron–Glia Interactions with the Brian 2 Simulator. In: De Pittà M., Berry H. (eds) Computational Glioscience. Springer Series in Computational Neuroscience. Springer, Cham.

[5] Tsodyks M (2005) Activity-dependent transmission in neocortical synapses. In: Chow C, Gutkin B, Hansel D, Meunier C, Dalibard, J (eds) Methods and models in neurophysics (Chap. 7). Elsevier, pp 245–265.